Monotonicity Properties and Spectral Characterization of Power Redistribution in Cascading Failures

Linqi Guo, Chen Liang and Steven H. Low Computing and Mathematical Sciences, California Institute of Technology, Pasadena, CA, 91125 Email:{lguo,cliang2,slow}@caltech.edu

Abstract—In this work, we apply spectral graph theory methods to study the monotonicity and structural properties of power redistribution in a cascading failure process. We demonstrate that in contrast to the lack of monotonicity in physical domain, there is a rich collection of monotonicity one can explore in the spectral domain, leading to a systematic way to define topological metrics that are monotonic. It is further shown that many useful quantities in cascading failure analysis can be unified into a spectral inner product, which itself is related to graphical properties of the transmission network. Such graphical interpretations precisely capture the Kirchhoff's law expressed in terms of graph structural properties and gauge the impact of a line when it is tripped. We illustrate that our characterization leads to a tree-partition of the network so that failure cascading can be localized.

I. INTRODUCTION

Power system reliability is a crucial part in the sustainable development of modern society. Recent blackouts, especially the 2003 and 2012 blackouts in Northwestern US [1] and India [2], demonstrated the devastating economic impact a grid failure can incur. In even worse cases where facilities like hospitals are involved, such blackouts pose threat directly to people's health and lives. Cascading failure of power grid components, especially the transmission lines, is the direct cause of blackouts.

Because of the delicate interactions among power system components, outages may cascade and propagate in a very complicated manner, and typically exhibit quite different patterns for different networks [3]. Such complexity originates from the interplay between network topology and Kirchhoff's law, and is aggravated by possible hidden failures and human errors involved. Existing work, roughly speaking, tackles this difficulty in three ways: i) by resorting to simulation models [4], which relies on Monte-Carlo simulations and accounts for the steady state power flow redistribution based on DC [5], [6] or AC [7], [8] model, with refinements including hidden failure [9], human erroneous response [5] etc.; ii) by studying pure topological models [10]–[12], which poses certain assumptions on the cascading dynamics (say failures

This work has been supported by NSF grants through CCF 1637598, ECCS 1619352, CNS 1545096, ARPA-E grants through award DE-AR0000699 (NODES) and GRID DATA, DTRA grant through HDTRA 1-15-1-0003 and Skoltech grant through collaboration agreement 1075-MRA.

propagate to adjacent lines with high probability) and infers component failure propagation patterns from graph-theoretic properties; iii) by investigating simplified cascading failure dynamics [13], [14]. It is often challenging to make general inferences across different scenarios due to the lack of understanding in structural properties of power redistribution.

Monotonic structures in a cascading failure process are usually helpful in outage mitigation. For instance, monotonicities are exploited in [15] to improve the computational efficiency for a load shedding policy. However, as pointed out by [16], monotonicity is the exception rather than the norm in power redistribution. For example, power flow over a specific branch can increase, decrease and even reverse direction as cascading failure unfolds [17]. The failure of a line can cause another line that is arbitrarily far away to be tripped [18]. Load shedding instead of mitigating the cascading failure, can actually increase the congestion on certain lines [19].

In this paper, we take a different approach from existing work to understand the monotonicity and structural properties of a cascading failure process. In particular, we demonstrate that in contrast to the lack of monotonicity in the physical domain, there is a rich collection of monotonicity one can explore in the spectral domain. This allows us to systematically design topological measures that are monotonic over the cascading event. Then we define a spectral inner product that unifies many useful quantities in existing cascading failure analysis. This inner product is inherently related to graph properties of the transmission network, revealing a graphical interpretation of the power redistribution. Such graphical interpretations, in contrast to the pure topological models in [10]-[12], do not rely on any assumptions or simplifications on how the failures propagate, but only reflect the Kirchhoff's law in a precise way. The graphical interpretations suggest a tree-partition of the grid network, which has the property that line failures can be localized into the decomposed regions. This partition can also be exploited to simplify and speed up the computation of the line outage redistribution factors [20] that are widely used in contingency analysis.

The rest of the paper is organized as follows. In Section II, we present the cascading failure model and review relevant concepts from spectral graph theory. In Section III, we collect and derive the basic properties of the Laplacian matrix under

the power redistribution setting. We then show there is a rich set of monotonicity in the spectrum of the Laplacian matrix in Section IV. In Section V, we show how an inner product from the spectral domain unifies several useful quantities in cascading failure analysis and relate them to graphical properties. In Section VI, we demonstrate that our characterization motivates a tree-partition of the network so that line failures can be localized and explain how such localization can be exploited to speed up the computation of line outage redistribution factors. We also present a counter-intuitive phenomenon on the impact of lines with high spanning tree centrality. We conclude in Section VII.

II. MODEL AND PROBLEM SETUP

In this section, we present our cascading failure model and review relevant concepts from spectral graph theory.

Let \mathbb{R} denote the set of real numbers. We reserve uppercase symbols like A, B, C for matrices. The bold symbol 1 denotes a vector of proper dimension whose entries are all 1. We also use u_i and u_{ij} to represent the vectors of proper dimension, with the *i*-th entry of u_i and u_{ij} being 1, the *j*-th entry of u_{ij} being -1, and all other entries being zero. A variable without subscript usually denotes a vector with appropriate components, e.g., $p = (p_i, i \in \mathcal{N})$. For any matrix A, we use A^{T} , A^{-1} , A^{\dagger} to represent its transpose, inverse and Moore-Penrose inverse, respectively. For a matrix A, \overline{A} means the matrix obtained from A by deleting either its last row or last column or both, depending on the context. For a vector v, we use $\operatorname{diag}(v)$ to denote the diagonal matrix with entries from v as main diagonal. The symbol t is reserved to represent the time index in the cascading process. A symbol with index tlike A(t) represents the corresponding quantity at time t.

We use the graph $\mathcal{G} = (\mathcal{N}^+, \mathcal{E})$ to describe the power transmission network before any line is tripped, where $\mathcal{N}=$ $\{1,\ldots,n-1\}$ is the set of non-slack buses, n is the slack bus, $\mathcal{N}^+ = \mathcal{N} \cup \{n\}$ and $\mathcal{E} \subset \mathcal{N}^+ \times \mathcal{N}^+$ denotes the set of transmission lines. The terms bus/node and line/edge are used interchangeably in this paper. An edge in \mathcal{E} is denoted either as e or (i, j). We further assign an arbitrary orientation over \mathcal{E} so that if $(i,j) \in \mathcal{E}$ then $(j,i) \notin \mathcal{E}$. The line reactance of e is denoted as x_e .

Our cascading failure model mainly focuses on the dynamics of line outages. More specifically, we consider a time horizon T of operation interest in the cascading process. At each time $t \in T$, there is a set of lines that are already tripped, which we denote as B(t). Let $\mathcal{E}(t) = \mathcal{E} \setminus B(t)$ be the set of remaining lines at time t, then the graph $\mathcal{G}(t) := (\mathcal{N}^+, \mathcal{E}(t))$ describes the active physical network at time t. In a cascading failure process, the set of tripped lines expand over time:

$$B(t) \subset B(t+1), \quad \forall t \in T$$

We assume that $\mathcal{G}(t)$ is connected and simple throughout the operation period, thus our analysis applies until the network breaks into islands. Once multiple islands are formed, we can apply our analysis separately to each component.

We denote the power injection, phase angle at bus i as $p_i(t)$ and $\theta_i(t)$ and denote the branch flow on link e as $P_e(t)$. The reactance matrix at time t is denoted as $X(t) = \operatorname{diag}(x_e : e \in$

 $\mathcal{E}(t)$). Let n, m(t) be the number of buses and transmission lines in $\mathcal{G}(t)$, respectively. The incidence matrix of $\mathcal{G}(t)$ is an $n \times m(t)$ matrix C(t) defined as

$$C_{ie}(t) = \begin{cases} 1 & \text{if node } i \text{ is the source of } e \\ -1 & \text{if node } i \text{ is the target of } e \\ 0 & \text{otherwise} \end{cases}$$

With above notations, the DC power flow model can be written

$$p(t) = C(t)P(t) \tag{1a}$$

$$p(t) = C(t)P(t)$$
 (1a)

$$X(t)P(t) = C(t)^{T}\theta(t)$$
 (1b)

where (1a) is the flow conservation constraint and (1b) is the Kirchhoff's and Ohm's law. At each time t, the power flow redistributes over the network described by $\mathcal{G}(t)$ according to the DC model (1). After the power flow stabilizes, lines are tripped based on certain rule, causing an expansion of the set of tripped lines B(t). Different tripping rules, for example the steady state deterministic rule [15], [16], the moving averaging rule [21], [22] and the stochastic rule [21], have been proposed in literature. We do not specialize to any of such rules as our structural results apply to all of them. A choice of tripping rule is only needed when one designs load shedding policy.

At each time $t \in T$, the (reactance weighted) graph Laplacian matrix of G(t) is the $n \times n$ symmetric matrix $L_{\mathcal{G}(t)} = C(t)X(t)^{-1}C^{T}(t)$, which is explicitly given by

$$L_{\mathcal{G}(t),ij} = \begin{cases} -x_{ij}^{-1} & i \neq j, (i,j) \text{ or } (j,i) \in \mathcal{E}(t) \\ \sum_{k \in N_i(t)} x_{ik}^{-1} & i = j \\ 0 & \text{otherwise} \end{cases}$$

where $N_i(t)$ is the set of neighbours of bus i in $\mathcal{G}(t)$. It is well known that if the graph $\mathcal{G}(t)$ is connected, then $L_{\mathcal{G}(t)}$ has rank n-1 and any principal submatrix of $L_{\mathcal{G}(t)}$ is invertible [23]. Let $\overline{L}_{\mathcal{G}(t)}$ be the matrix obtained from $L_{\mathcal{G}(t)}$ by deleting its last row and column, which corresponds to removing the slack bus. Then we see the matrix $A_{\mathcal{G}(t)} := \left(\overline{L}_{\mathcal{G}(t)}\right)^{-1}$ is always well-defined.

As will be shown in Section III, the matrix $A_{\mathcal{G}(t)}$ and the Moore-Penrose inverse of $L_{\mathcal{G}(t)}$, denoted as $L_{\mathcal{G}(t)}^{\uparrow}$, are useful when solving P(t) from the DC model (1). It is tempting to conclude $A_{\mathcal{G}(t)} = L_{\mathcal{G}(t)}^{\dagger}$, that is $A_{\mathcal{G}(t)}$ is a submatrix of $L_{\mathcal{G}(t)}^{\dagger}$. This, however, is not true in general. Nevertheless, we show in Section III that they are closely related in a precise way.

III. BASIC PROPERTIES

In this section, we review and derive basic properties of the matrices defined in Section II. For presentation clarity, we drop the time index t and subscripts $\mathcal{G}(t)$ from our notations.

Let us first look at the Laplacian matrix L. For any $v \in \mathbb{R}^n$, we can compute

$$v^{T}Lv = \sum_{(i,j)\in\mathcal{E}} x_{ij}^{-1} (v_i - v_j)^2 \ge 0$$
 (2)

Thus L is positive semidefinite and hence diagonalizable. Moreover, equation (2) also implies the kernel of L is span $(\{1\})$, the set of vectors with uniform entries.

The Laplacian matrix L appears in circuit analysis as the admittance matrix (with a different weight), which explicitly relates the voltage and current vector in a pure resistive network [24]. It is shown in [24] that the effective resistance between two nodes i and j can be computed as

$$R_{ij} := L_{ii}^{\dagger} + L_{jj}^{\dagger} - L_{ij}^{\dagger} - L_{ji}^{\dagger} \tag{3}$$

Following a similar calculation, we can show that (3) gives the effective reactance between the buses i and j for the power network. That is, assuming we connect the buses i and j to an external probing circuit, when there is no other injection in the network, the power flow P_{ij} (from the external circuit) into bus i and out from bus j (into the external circuit) is given as

$$P_{ij} = \frac{\theta_i - \theta_j}{R_{ij}}$$

and therefore the network can be equivalently reduced to a single line with reactance R_{ij} . When i and j are directly connected, physical intuition suggests

$$R_{ij} < x_{ij}$$

as connection from the network can only decrease the overall reactance. We show in Section V that $x_{ij} - R_{ij}$ also carries graphical meaning, proving its nonnegativity rigorously.

Next, we derive explicit formula for the branch flow vector P in terms of the power injection p, from which we derive a relation between $\overline{L^\dagger}$ and A. Substituting (1b) to (1a) we obtain $p=L\theta$. Therefore if $\mathbf{1}^Tp=0$, the solution θ is unique after quotient away the kernel span ($\{\mathbf{1}\}$). Noting this is also the kernel of C^T , we see that $P=X^{-1}C^T\theta$ is uniquely determined. Towards the goal of an explicit formula, we can proceed in two ways. The first way relies on the fact that $L^\dagger p$ always gives a feasible θ and therefore

$$P = X^{-1}C^T L^{\dagger} p \tag{4}$$

The second way is to set the phase angle at the slack bus to zero, which implies that

$$\overline{\theta} = \overline{L}^{-1} \overline{p} = A \overline{p}$$

where $\overline{\theta}$ and \overline{p} are the vector of non-slack bus phase angles and injections. Denote by \overline{C} the matrix obtained from removing the last row of C, we then have

$$P = X^{-1} \overline{C}^T \overline{\theta} = X^{-1} \overline{C}^T A \overline{p}$$
 (5)

Consider a line $(i,j) \in \mathcal{E}$ with neither i nor j being the slack bus. Under the injection $p_i = -p_j = 1$, by equating the branch flow P_{ij} computed from (4) and (5), we obtain that

$$L_{ii}^{\dagger} + L_{jj}^{\dagger} - L_{ij}^{\dagger} - L_{ji}^{\dagger} = A_{ii} + A_{jj} - A_{ij} - A_{ji}$$
 (6)

This tells us although A and $\overline{L^\dagger}$ are generally not the same, they do satisfy the equation (6). It turns out that L^\dagger is more amenable to monotonic analysis for procedural properties, as in Section IV, and A is easier to manipulate when we derive one-step results for power redistribution, as in Section V. Equation (6) precisely relates results of these two types.

IV. SPECTRAL MONOTONICITY

In this section, we present our results for monotonicity in cascading failure processes. Our characterization is related to known monotonicity results and suggests a systematic way to define monotonic topological metrics over a failure event.

Our approach focuses on the Laplacian spectrum of the system. In contrast to the lack of monotonicity in the physical system, when we look at the process from the spectral domain, there is in fact a rich set of monotonicity one can explore. They are built upon the following fundamental monotonicity result.

Theorem IV.1. Let $\lambda_1(t) \leq \lambda_2(t) \leq \cdots \leq \lambda_n(t)$ be the eigenvalues of $L_{\mathcal{G}(t)}$. Then $\lambda_i(t)$ is a decreasing function in t for each i. Moreover, for each t, as long as new lines are tripped at time t, there exists i such that the decrease is strict

$$\lambda_i(t+1) < \lambda_i(t)$$

The Laplacian eigenvalues usually encode information on how well the graph is connected and how fast information can propagate in the network, see [25] for example. Therefore this result tells us that, as the cascading failure process unfolds, there is a decreasing level on the network connectivity and its "mixing ability". Theorem IV.1 can be interpreted as a fundamental property for the network topology during the cascading process, which is independent of the specific power flow dynamics and failure propagation patterns. Although this result only reflects the network topology evolution, we demonstrate in Corollary IV.6 that by applying such monotonicity properly, it is possible to devise monotonic properties that are directly related to the power flow dynamics.

To prove Theorem IV.1, we first derive an eigenvalue interlacing result for generic weighted Laplacian matrices. Its special case where the graph is unweighted and only a single line is removed is known in literature [26].

Proposition IV.2. Let \mathcal{G} be a weighted graph with positive line weights $\{w_e\}$ and let \mathcal{H} be a subgraph of \mathcal{G} obtained by removing exactly s edges from \mathcal{G} . Denote $\lambda_1 \leq \lambda_2 \leq \ldots \leq \lambda_n$ and $\mu_1 \leq \mu_2 \leq \ldots \leq \mu_n$ to be the eigenvalues of $L_{\mathcal{G}}$ and $L_{\mathcal{H}}$, respectively. Then for any $k = 1, 2, \ldots, n$, we have

$$\mu_k \le \lambda_k \tag{7}$$

and for $k = s + 1, s + 2, \dots, n$, we have

$$\lambda_{k-s} \le \mu_k \tag{8}$$

As an immediate corollary, we can deduce the following well known result for s=1.

Corollary IV.3. With previous notations, when \mathcal{H} is obtained by removing a single edge from \mathcal{G} , we have

$$\mu_1 \le \lambda_1 \le \mu_2 \le \dots \le \lambda_{n-1} \le \mu_n \le \lambda_n$$

We now specialize the generic weighted Laplacian matrix in Proposition IV.2 to the reactance weighted Laplacian matrix as defined in Section II. Note that in a cascading process described by the graph sequence $\{\mathcal{G}(t)\}_{t\in T},\ \mathcal{G}(t+1)$ is obtained from $\mathcal{G}(t)$ by removing the tripped lines incurred during time t. Therefore from Proposition IV.2 we know the

functions $\lambda_i(t)$ as defined in Theorem IV.1 are monotonically decreasing.

Proof of Theorem IV.1. Based on the previous discussion, it suffices to show that for each t, we can always find i such that the decrease is strict. But this is immediate after noting

$$\sum_{i} \lambda_{i}(t+1) = \operatorname{tr}(L_{\mathcal{G}(t+1)}) = \sum_{e \in \mathcal{E}(t+1)} x_{e}^{-1}$$

$$< \sum_{e \in \mathcal{E}(t)} x_{e}^{-1} = \operatorname{tr}(L_{\mathcal{G}(t)})$$

$$= \sum_{i} \lambda_{i}(t)$$

where the inequality is strict because there are lines tripped at time t.

Such monotonicity of Laplacian eigenvalues suggests that all metrics measuring the system from its spectrum should be monotonic as well. The most general result we can conclude along this line is the following.

Corollary IV.4. Let $\| \cdot \|$ be a unitarily-invariant norm on the set of $n \times n$ matrices. Then $\| L_{\mathcal{G}(t)} \|$ is a decreasing function of t.

Proof. This is an immediate result from the bijective correspondence between unitarily invariant norms on $n \times n$ matrices and symmetric gauge functions applied to the matrix singular values [27], because symmetric gauge functions are monotone in the vector components.

Examples of unitarily-invariant norms include the spectral norm, nuclear norm, Frobenious norm, Schatten p-norms and Ky-Fan k-norms etc., each of which suggests a different way to measure the system monotonicity. For example, the monotonicity in nuclear norm recovers the fact that the sum of all link reactances decreases in a cascading failure process.

It is well-known from singular value decomposition that the nonzero eigenvalues of $L^\dagger_{\mathcal{G}(t)}$ are given as $1/\lambda_i(t)$, with the same corresponding eigenvectors as $L_{\mathcal{G}(t)}$. Therefore Theorem IV.1 implies the eigenvalues of $L^\dagger_{\mathcal{G}(t)}$ are monotonically increasing. It is tempting to conclude from this fact that $v^T L^\dagger_{\mathcal{G}(t)} v$ is monotonically increasing for a fixed $v \in \mathbb{R}^n$, but the situation becomes tricky after we notice that the eigenvectors of $L_{\mathcal{G}(t)}$ also evolve with t. Fortunately, we can still prove such monotonicity with careful algebra.

Proposition IV.5. For any $v \in \mathbb{R}^n$, the function $V(t) := v^T L_{G(t)}^{\dagger} v$ is increasing in t.

Proof. Without loss of generality, let us assume there is only a single edge (i, j) tripped at time t. The general case follows by tripping the lines one by one.

Under such assumption, by direct computation we have

$$L_{\mathcal{G}(t+1)} = L_{\mathcal{G}(t)} - x_{ij}^{-1} u_{ij} u_{ij}^{T}$$

It is shown in [15] that this rank one perturbation translates in its Moore-Penrose inverse to the equation

$$L_{\mathcal{G}(t+1)}^{\dagger} = L_{\mathcal{G}(t)}^{\dagger} + \frac{1}{x_{ij} - R_{ij}} L_{\mathcal{G}(t)}^{\dagger} u_{ij} u_{ij}^{T} L_{\mathcal{G}(t)}^{\dagger}$$
(9)

where R_{ij} is the effective reactance between bus i and j defined in (3). Recall we always have $x_{ij} - R_{ij} > 0$ for directly connected i and j (as long as after removing (i,j), the network is still connected), we thus see the second term in (9) is positive semidefinite. The monotonicity of V(t) then follows.

The network tension [16] at time t is defined to be $H(t) = P(t)^T X(t) P(t)$, which measures the aggregate load of the network and is shown to be an increasing function of t in [16]. We now show this is a special case of our result.

Corollary IV.6. H(t) is an increasing function in t.

Proof. We can calculate that (for notation simplicity, we drop the subscript t)

$$\begin{split} P^TXP &= p^TL_{\mathcal{G}}^{\dagger}MX^{-1}XX^{-1}M^TL_{\mathcal{G}}^{\dagger}p \\ &= p^TL_{\mathcal{G}}^{\dagger}L_{\mathcal{G}}L_{\mathcal{G}}^{\dagger}p \\ &= p^TL_{\mathcal{C}}^{\dagger}p \end{split}$$

By Proposition IV.5 we then know H(t) is monotonically increasing. \Box

The equation (9) not only shows the monotonicity of H(t), but also implies the precise increment of H(t) at each t is inversely proportional to the amount of reactance reduction of (i,j) from the network at time t. Such reduction is in fact closely related to the spanning tree centrality [28] of (i,j), as we explain in Section V.

V. SPECTRAL INNER PRODUCT

In this section we define an inner product in the spectral domain and explain how it relates power redistribution to graphical properties. Our result in this section is for power redistribution in one step, thus we drop the time index t and subscript $\mathcal{G}(t)$ from all the notations.

For a real function defined on \mathcal{N} , we can identify it with a vector in \mathbb{R}^{n-1} . The correlation of two functions defined on the non-slack buses can thus be measured by inner products between the corresponding vectors in \mathbb{R}^{n-1} . It turns out that a particularly informative inner product in our application is from the spectral domain, defined as follows.

Definition V.1. For any two vectors $x, y \in \mathbb{R}^{n-1}$, their spectral inner product is defined as

$$\langle x,y\rangle_A=x^TAy$$

It is straightforward to check that $\langle \cdot, \cdot \rangle_A$ defines an inner product as A is symmetric and positive definite. To see why it is called the spectral inner product, let $\mu_1 \leq \mu_2 \leq \cdots \leq \mu_{n-1}$ be the eigenvalues of A with corresponding orthonormal eigenvectors $v_1, v_2, \ldots, v_{n-1}$. Then we have

$$\langle x, y \rangle_A = \sum_{k=1}^{n-1} \mu_k(x^T v_k)(y^T v_k)$$

Recall A and \overline{L} share the same eigenvectors as they are inverse of each other. We thus see that for x and y, $\langle x,y\rangle_A$ is the inner product of their spectral representations scaled by the corresponding eigenvalues.

The significance of this spectral inner product is twofold. First, many useful quantities in cascading failure analysis can be expressed as the spectral inner product of the corresponding indicator functions, which we will define shortly. Second, the spectral inner product carries explicit meaning in the graphical structures of the underlying network, giving topological interpretations of such spectral correlation. This relates structural properties in power redistribution to graphical properties of the physical network and reveals the precise measure to gauge the impact of certain buses/lines in a cascading failure process.

To elaborate on the first point, let us see how the spectral inner product unifies some useful quantities. For a bus $i \in \mathcal{N}$ and line $(k,j) \in \mathcal{E}$, we say $u_i \in \mathbb{R}^{n-1}$ and $u_{jk} \in \mathbb{R}^{n-1}$ are their indicator functions respectively. Such association is natural and turns out to be useful. Indeed, by (6), we see the effective reactance of an line (i,j) can be rewritten as

$$R_{ij} = \langle u_{ij}, u_{ij} \rangle_A$$

which is the squared induced norm of its indicator function. As another example, we can examine the generation shift sensitivity factor [20], denoted as D_{ie} , which measures how much the change in the injection to bus i affects the branch flow on line e. Denote e=(j,k) with $j,k\in\mathcal{N}$, then [20] computed $D_{ie}=A_{ij}-A_{ik}$. Using the spectral inner product, we can simply write

$$D_{ie} = \langle u_i, u_{jk} \rangle_A$$

which is the spectral correlation between the indicator functions of bus i and edge e.

The most relevant quantity in understanding the power redistribution in a cascading failure process is the line outage redistribution factor [20], which we denote as $K_{e\hat{e}}$. When the line e is tripped, $K_{e\hat{e}}$ is the ratio between the branch flow change over line \hat{e} and the original branch flow on e before it is tripped. Writing $e=(i,j), \hat{e}=(w,z)$ with $i,j,w,z\in\mathcal{N}$, the constant $K_{e\hat{e}}$ is explicitly given as [20]

$$K_{e\hat{e}} = \frac{x_e}{x_{\hat{e}}} \frac{A_{iw} + A_{jz} - A_{jw} - A_{iz}}{x_e - (A_{ii} + A_{jj} - A_{ij} - A_{ij})}$$

which can be rewritten using spectral inner product into

$$K_{e\hat{e}} = \frac{x_e}{x_{\hat{e}}} \frac{\langle u_{ij}, u_{wz} \rangle_A}{x_e - \langle u_{ij}, u_{ij} \rangle_A}$$
(10)

This quantity is proportional to the spectral correlation between the indicator functions of e and \hat{e} , and is inversely proportional to the reactance reduction $x_{ij} - R_{ij}$.

To facilitate our discussion on the second point, more notations are in order. Given a subset E of \mathcal{E} , we use \mathcal{T}_E to denote the set of spanning trees of \mathcal{G} with edges from E. For two subsets $\mathcal{N}_1, \mathcal{N}_2$ of \mathcal{N}^+ , we define $\mathcal{T}(\mathcal{N}_1, \mathcal{N}_2)$ to be the set of spanning forests of \mathcal{G} consisting of exactly two trees that contain \mathcal{N}_1 and \mathcal{N}_2 respectively. See Fig. 1 for an illustration of $\mathcal{T}(\mathcal{N}_1, \mathcal{N}_2)$. Given a set E of edges, we write

$$\chi(E) := \prod_{e \in E} x_e^{-1}$$

Then the celebrated All Minors Matrix Tree Theorem [29] applied to the matrix \overline{L} implies

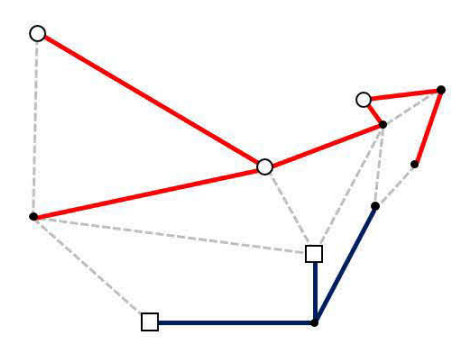


Fig. 1. An example element in $\mathcal{T}(\mathcal{N}_1, \mathcal{N}_2)$, where circles correspond to elements in \mathcal{N}_1 and squares correspond to elements in \mathcal{N}_2 . The two spanning trees containing \mathcal{N}_1 and \mathcal{N}_2 are highlighted as solid lines.

Proposition V.2. The determinant of the matrix obtained by deleting the *i*-th row and *j*-th column of \overline{L} , denoted as \overline{L}^{ij} , is given by

$$\det\left(\overline{L}^{ij}\right) = (-1)^{i+j} \sum_{E \in \mathcal{T}(\{i,j\},\{n\})} \chi(E)$$

This leads to the following graphical interpretation of the spectral inner product.

Proposition V.3. For any $i, j \in \mathcal{N}$, we have

$$\left\langle u_i, u_j \right\rangle_A = \frac{\sum_{E \in \mathcal{T}(\{i,j\},\{n\})} \chi(E)}{\sum_{E \in \mathcal{T}_{\mathcal{E}}} \chi(E)}$$

Therefore the spectral inner product captures the graph topological information on its spanning tree distribution. The practical meaning of such interpretation in power redistribution setting will be clear in Theorem V.6. Before that, we first present two corollaries revealing graphical interpretations of the aforementioned quantities.

Corollary V.4. For $i, j \in \mathcal{N}$, we have

$$x_{ij} - R_{ij} = x_{ij} \cdot \frac{\sum_{E \in \mathcal{T}_{\mathcal{E} \setminus \{(i,j)\}}} \chi(E)}{\sum_{E \in \mathcal{T}_{\mathcal{E}}} \chi(E)}$$

In particular, we always have $x_{ij} \geq R_{ij}$ and the inequality is strict if the graph after removing (i,j) is connected.

This result tells us that for an edge (i, j), the reduction ratio of its reactance coming from the network is exactly given as the (weighted) portion of spanning trees not passing through (i, j) among all spanning trees. Thus more connection from the network leads to more reduction in the effective reactance on (i, j), which agrees with our physical intuition.

We remark that this reactance reduction ratio is closely related to the spanning tree centrality measure [30]. Indeed, from the very definition of spanning tree centrality, we have

$$\frac{\sum_{E \in \mathcal{T}_{\mathcal{E}} \setminus \{(i,j)\}} \chi(E)}{\sum_{E \in \mathcal{T}_{\mathcal{E}}} \chi(E)} + c_{(i,j)} = 1$$

where $c_{(i,j)}$ denotes the spanning tree centrality of (i,j). This implies that

$$R_{ij} = x_{ij}c_{(i,j)}$$

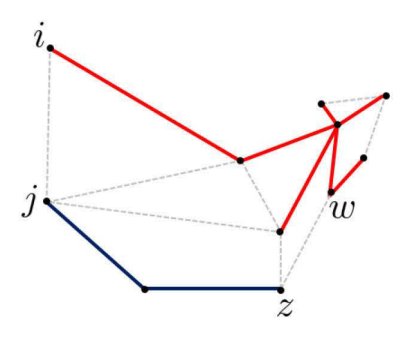


Fig. 2. An example element in $\mathcal{T}(\{i,w\},\{j,z\})$. The spanning trees containing $\{i,w\}$ and $\{j,z\}$ are highlighted as solid lines.

or in other words, in a power redistribution setting, the spanning tree centrality precisely captures the ratio of effective reactance compared to the line reactance. In fact, this relation (or more precisely the effective resistance counterpart) is the theoretical foundation for the state-of-the-art algorithm in computing spanning tree centrality measures. See [28] for more details.

Corollary V.5. For $i, j, w, z \in \mathcal{N}$, we have

$$\langle u_{ij}, u_{wz} \rangle_A = \frac{1}{\sum_{E \in \mathcal{T}_{\mathcal{E}}} \chi(E)} \left(\sum_{E \in \mathcal{T}(\{i, w\}, \{j, z\})} \chi(E) - \sum_{E \in \mathcal{T}(\{i, z\}, \{j, w\})} \chi(E) \right)$$

Note that (i,j) and (w,z) are not required to be lines in \mathcal{E} in this result. When e=(i,j) and $\hat{e}=(w,z)$ are indeed lines in \mathcal{E} , the above quantity reduces to the spectral correlation of e and \hat{e} . As we will discuss shortly, the sign of this spectral correlation in fact fully determines the sign of $K_{e\hat{e}}$. Similar formula for D_{ie} can be deduced, which we omit here in light of space limitation.

We are now ready to derive an alternative formula for $K_{e\hat{e}}$.

Theorem V.6. Let $e=(i,j), \hat{e}=(w,z)$ be edges with $i,j,w,z \in \mathcal{N}$. We have

$$K_{e\hat{e}} = \frac{1}{x_{\hat{e}}} \frac{\sum_{E \in \mathcal{T}(\{i,w\},\{j,z\})} \chi(E) - \sum_{E \in \mathcal{T}(\{i,z\},\{j,w\})} \chi(E)}{\sum_{E \in \mathcal{T}_{\mathcal{E} \setminus \{(i,j)\}}} \chi(E)}$$
(11)

Proof. This follows from dividing the equation in Corollary V.5 by the equation in Corollary V.4. \Box

Despite the complexity of (11), all terms in this formula carry clear meanings, as we now explain.

We first focus on the numerator of (11), in which the sum is over the spanning forests $\mathcal{T}(\{i,w\},\{j,z\})$ and $\mathcal{T}(\{i,z\},\{j,w\})$. Each element in $\mathcal{T}(\{i,w\},\{j,z\})$, as illustrated in Fig. 2, specifies a way to connect i to w and j to z through trees and captures a possible path for edge (i,j) to "spread" impact to (w,z). Similarly, elements in $\mathcal{T}(\{i,z\},\{j,w\})$ captures possible paths for edge (i,j) to

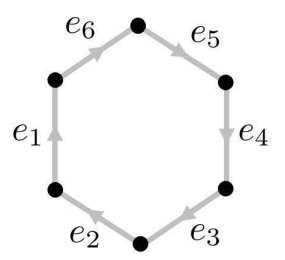


Fig. 3. A ring network with clockwise orientation.

"spread" impact to (z,w), which counting orientation, contributes negatively to $K_{e\hat{e}}$. Therefore the numerator in (11) says that in power redistribution, the impact of line e is passed to \hat{e} through all possible spanning tree paths connecting e and \hat{e} , counting orientation. The relative strength of the positive and negative impacts determines the sign of $K_{e\hat{e}}$.

Comparing (11) and Corollary V.5, we see that the signs of $K_{e\hat{e}}$ and $\langle e,\hat{e}\rangle_A$ are the same¹. Thus the spectral correlation between two edges precisely captures the relative strength of the positive and negative impacts from e to \hat{e} . When the two impacts are of equal strength, e and \hat{e} are spectrally orthogonal. Such intuition allows us to decide the sign of $K_{e\hat{e}}$ in certain cases without any computation. For example, in the ring network shown in Fig. 3, by inspecting the graph, we conclude that

$$K_{e_1e_s} < 0, \quad s = 2, 3, 4, 5, 6$$

as e_1 can only spread negative impacts to other lines.

Now we focus on the denominator of (11), in which the sum is over all spanning trees that do not pass through (i,j). Each tree of this type specifies an alternative path that power can flow through if (i,j) is tripped. When there are more trees of this type, the network has better ability in absorbing the impact of (i,j) being tripped. Therefore the denominator of (11) precisely says that the impact of (i,j) being tripped to other lines is inversely proportional to the sum of all alternative tree paths in the network. The $1/x_{\ell}$ constant in (11) captures the intuition that lines with larger reactance tend to be more robust against failures of other lines.

The formula (11) does not exhibit computational advantage comparing to existing numerical methods for computing $K_{e\hat{e}}$. The significance of this result lies in its implication in structural properties of power flow redistribution and the fact that it allows us to make general inferences by simply looking at the network topology. As an example, we deduce the following result from (11), which is also shown in [16], but with longer proof.

Corollary V.7. For adjacent lines e = (i, j) and $\hat{e} = (i, k)$ with $i, j, k \in \mathcal{N}$, we have

$$K_{e\hat{e}} > 0$$

Proof. For such e and \hat{e} , the negative term in the numerator of (11) is over the empty set and thus equals to 0.

¹We overload the notation $\langle e, \hat{e} \rangle_A$ to represent $\langle u_{ij}, u_{wz} \rangle_A$, where e = (i,j) and $\hat{e} = (w,z)$.

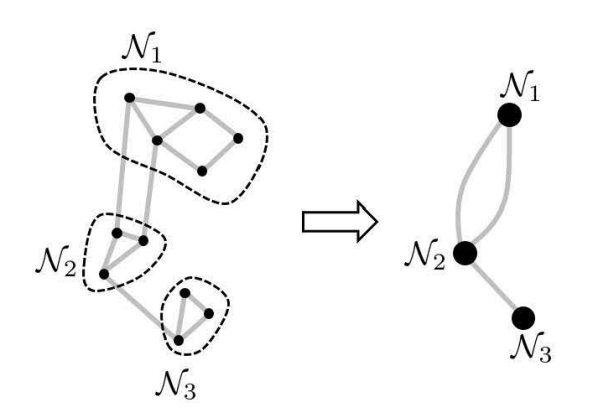


Fig. 4. An illustration of the reduced graph $\mathcal{G}_{\mathcal{P}}$. This is NOT a tree-partition due to the multiple lines between \mathcal{N}_1 and \mathcal{N}_2 .

VI. APPLICATIONS

In this section, we demonstrate two applications of our characterization (11).

A. Tree-partition for failure localization

We present a type of graph partition motivated by (11), which has the property that line failure impacts over a cascading event can be localized. Given a network $\mathcal{G} = (\mathcal{N}^+, \mathcal{E})$, we say a collection $\mathcal{P} = \{\mathcal{N}_1, \mathcal{N}_2, \cdots, \mathcal{N}_k\}$ of subsets of \mathcal{N}^+ forms a partition of \mathcal{G} , if $\mathcal{N}_i \cap \mathcal{N}_j = \emptyset$ for $i \neq j$ and $\cup_{i=1}^k \mathcal{N}_i = \mathcal{N}^+.$ For any partition, we can define a reduced multi-graph $\mathcal{G}_{\mathcal{P}}$ as follows. First, we reduce each subset \mathcal{N}_i to a super node. The set of all super nodes forms the node set for $\mathcal{G}_{\mathcal{P}}$. Second, we add a line connecting super nodes \mathcal{N}_i and \mathcal{N}_i for each pair of n_i, n_j with the property that $n_i \in \mathcal{N}_i, n_j \in \mathcal{N}_j$ and n_i and n_j are connected in \mathcal{G} . See Fig. 4 for an illustration. We say a partition \mathcal{P} is a *tree-partition* if the reduced graph $\mathcal{G}_{\mathcal{P}}$ is a tree. When this is the case, for $n_i \in \mathcal{N}_i, n_i \in \mathcal{N}_i$ such that $(n_i, n_j) \in \mathcal{E}$, the line (n_i, n_j) is said to be a bridge connecting \mathcal{N}_i and \mathcal{N}_i . When a line has both of its end points in \mathcal{N}_i , we say the line itself is in \mathcal{N}_i .

The significance of a tree-partition lies in the fact that for such partition, when a line in \mathcal{N}_i is tripped, all lines in \mathcal{N}_j with $j \neq i$ are not affected and therefore the failure is localized. We remark that such localization only holds until the network becomes disconnected, because a line failure in \mathcal{N}_i that disconnects the network can cause branch flow changes in bridge lines connecting \mathcal{N}_i and \mathcal{N}_j , which then indirectly cause branch flow changes for lines in \mathcal{N}_i .

To see why the failure can be localized, we first pick two arbitrary bus subsets from \mathcal{P} . Without loss of generality, we assume the two subsets are \mathcal{N}_1 and \mathcal{N}_2 . Let $e=(i,j)\in\mathcal{N}_1$ and $\hat{e}=(w,z)\in\mathcal{N}_2$ with $i,j,w,z\in\mathcal{N}$. We now show $K_{e\hat{e}}=0$. Indeed, since \mathcal{P} is a tree-partition, any path from i to w must go through all bridge lines on the path from \mathcal{N}_1 to \mathcal{N}_2 in the reduced graph $\mathcal{G}_{\mathcal{P}}$. The situations for any path from j to z, from i to z and from z to z are similar. This implies $\mathcal{T}(\{i,w\},\{j,z\})=\mathcal{T}(\{i,z\},\{j,w\})=\emptyset$. By (11), we then know $K_{e\hat{e}}=0$, or in other words, when z is tripped, the branch flow on z does not change. Next, for each bridge

line, because of the power conservation (1a), its branch flow is uniquely determined by the aggregate injections of all super nodes. Therefore, as long as the network $\mathcal G$ is still connected and thus the aggregate injections at all super nodes remain the same, the branch flows on all bridge lines are unchanged. As a result, the failure localization holds until the network $\mathcal G$ becomes disconnected.

A direct benefit of finding a tree-partition is that we can skip the computation of $K_{e\hat{e}}$ for e and \hat{e} in different partition regions. This benefit can be tremendous even for a coarse partition. For example, given a network with m edges, if we can find a tree-partition that divides the edges roughly equally to two regions so that each region contains about m/2 edges, then we can skip $2 \times \frac{m}{2} \times \frac{m}{2} = \frac{m^2}{2}$ many computations of $K_{e\hat{e}}$, about a half of all pairs of $K_{e\hat{e}}$ (note that $K_{e\hat{e}}$ is generally not symmetric in e and \hat{e}). If we can find a tree-partition that separates the lines roughly equally to k regions, a similar calculation shows that about 1-1/k portion of the calculation of $K_{e\hat{e}}$ can be skipped. Moreover, a tree-partition \mathcal{P} for $\mathcal{G}(0)$ is also a tree-partition for $\mathcal{G}(t)$ for any $t \in T$, thus the calculation of a good \mathcal{P} incurs only a one-time computation effort, but comes with the reward of skipping a significant computation time for $K_{e\hat{e}}$ over the whole operation period.

Although this localization phenomenon is only until the graph becomes disconnected, it guarantees that in a contingency scenario, the partitioned regions are independent from each other for at least a short period. This can be crucial as it creates a window that allows load-shedding control to take over in time and prevents more severe failures from happening. A subtle point suggested by this phenomenon is that in practice, even for the purpose of secure operation of the grid, it can be beneficial to deactivate certain transmission lines between major geographical regions so that a tree-partition of good quality can be formed. This not only localizes the impact of line failures to its own region, but also clearly implies the remaining bridge lines are the key components we should protect, allowing budget to be more purposefully spent.

B. Counter-intuitive Impact of Critical Line Reactance

It is tempting to conclude from (11) that the reactance of a line with more spanning trees passing through tends to have impacts on $K_{e\hat{e}}$ for more e and \hat{e} pairs because such reactance appears in the denominator term more often. Indeed, spanning tree centrality as a measure on line importance seems to also support this conjecture. We now, however, argue that (11) in fact leads to almost the opposite conclusion.

To illustrate this, we consider the limiting case where all spanning trees pass through a line \tilde{e} . Now pick arbitrary edges e=(i,j) and $\hat{e}=(w,z)$ and let us look at the spanning forests $\mathcal{T}(\{i,w\},\{j,z\})$. Note that for each element in $\mathcal{T}(\{i,w\},\{j,z\})$, by adding the edge e=(i,j), we can form a spanning tree of the whole network \mathcal{G} . Since all spanning trees pass through \tilde{e} , we see \tilde{e} must be part of every spanning forest in $\mathcal{T}(\{i,w\},\{j,z\})$, which implies that the reactance of \tilde{e} appears in $\sum_{E\in\mathcal{T}(\{i,w\},\{j,z\})}\chi(E)$ as a common factor. Similar argument applies to $\sum_{E\in\mathcal{T}(\{i,z\},\{j,w\})}\chi(E)$. Finally, the denominator of (11) also has the reactance of \tilde{e} as a common factor since all spanning trees pass through

 \tilde{e} . Therefore, the reactance of \tilde{e} is cancelled out and does not impact $K_{e\hat{e}}$ at all. This limiting case argument can be generalized and suggest that the reactance of lines with high spanning tree centrality in fact has small impact on how the cascading failure propagates in other parts of the network.

This, of course, does not imply that such lines are not important. Indeed, for a line with all spanning trees passing through, it is always a bridge line as we defined in Section VI-A, and therefore its removal results in the whole network being disconnected. What this counter-intuitive fact does imply is that the spanning tree centrality measure itself is not sufficient to identify the key components from a cascading failure perspective. The spectral correlations among the lines also play an important role.

VII. CONCLUSION

In this work, we study the monotonicity and structural properties of power redistribution in a cascading failure process. We demonstrate that there is a rich collection of monotonicity one can explore in the spectral domain and many useful quantities can be unified into a spectral inner product, which relates these quantities to graphical properties of the transmission network in a precise way. Our characterization can be used to speed up the computation of line outage redistribution factors for the sake of secure grid operation.

There are several future directions for this work. First, as we have shown in Section IV, a general class of quadratic forms are monotonic in a cascading failure process. It is of interest to see whether we can capture some important metrics about the grid by choosing v properly. Second, the spectral inner product has rich structures from a pure mathematical perspective such as Cauchy-Schwarz inequality. It can be useful to understand how such mathematical properties translate into intuition in a power redistribution setting. Third, to our best knowledge, the problem of finding a good tree-partition as we defined in Section VI-A has not been studied in either graph-theoretic or algorithm design community. It will be useful if this problem can be more systematically studied and a general purpose algorithm can be devised. Finally, we are still investigating how our understanding in such structural properties can help us design optimal load shedding policies.

REFERENCES

- [1] "U.s.-canada power system outage task force. report on the august 14, 2003 blackout in the united states and canada: Causes and recommendation" 2004.
- "Report of the enquiry committee on grid disturbance in northern region on 30th july 2012 and in northern, eastern and north-eastern region on 31st july 2012," Aug 2012.
- [3] S. Soltan, D. Mazauric, and G. Zussman, "Analysis of failures in power grids," IEEE Transactions on Control of Network Systems, vol. PP, no. 99, pp. 1-1, 2015.
- [4] I. Dobson, B. A. Carreras, V. E. Lynch, and D. E. Newman, "Complex systems analysis of series of blackouts: Cascading failure, critical points, and self-organization," Chaos: An Interdisciplinary Journal of Nonlinear Science, vol. 17, no. 2, p. 026103, 2007.
- [5] B. A. Carreras, V. E. Lynch, I. Dobson, and D. E. Newman, "Critical points and transitions in an electric power transmission model for cascading failure blackouts," Chaos: An interdisciplinary journal of nonlinear science, vol. 12, no. 4, pp. 985-994, 2002.
- [6] M. Anghel, K. A. Werley, and A. E. Motter, "Stochastic model for power grid dynamics," in System Sciences, 2007. HICSS 2007. 40th Annual Hawaii International Conference on. IEEE, 2007, pp. 113-113.

- [7] D. P. Nedic, I. Dobson, D. S. Kirschen, B. A. Carreras, and V. E. Lynch, "Criticality in a cascading failure blackout model," International Journal of Electrical Power & Energy Systems, vol. 28, no. 9, pp. 627-633, 2006.
- [8] M. A. Rios, D. S. Kirschen, D. Jayaweera, D. P. Nedic, and R. N. Allan, "Value of security: modeling time-dependent phenomena and weather conditions," IEEE Transactions on Power Systems, vol. 17, no. 3, pp. 543-548, 2002.
- [9] J. Chen, J. S. Thorp, and I. Dobson, "Cascading dynamics and mitigation assessment in power system disturbances via a hidden failure model," International Journal of Electrical Power & Energy Systems, vol. 27, no. 4, pp. 318-326, 2005.
- [10] A. E. Motter and Y.-C. Lai, "Cascade-based attacks on complex networks," Phys Rev E, Dec. 2002.
- [11] C. D. Brummitt, R. M. DSouza, and E. A. Leicht, "Suppressing cas-cades of load in interdependent networks," Proceedings of the National Academy of Sciences, vol. 109, no. 12, pp. E680-E689, 2012.
- [12] Z. Kong and E. M. Yeh, "Resilience to degree-dependent and cascading node failures in random geometric networks," IEEE Transactions on Information Theory, vol. 56, no. 11, pp. 5533-5546, Nov 2010.
- [13] C. L. DeMarco, "A phase transition model for cascading network
- failure," *IEEE Control Systems*, vol. 21, no. 6, pp. 40–51, Dec 2001. [14] I. Dobson, B. A. Carreras, and D. E. Newman, "A loading-dependent model of probabilistic cascading failure," Probab. Eng. Inf. Sci., vol. 19, no. 1, pp. 15-32, Jan. 2005.
- Q. Ba and K. Savla, "A dynamic programming approach to optimal load shedding control of cascading failure in dc power networks," in 2016 IEEE 55th Conference on Decision and Control (CDC), Dec 2016, pp.
- [16] C. Lai and S. H. Low, "The redistribution of power flow in cascading failures," in 2013 51st Annual Allerton Conference on Communication, Control, and Computing (Allerton), Oct 2013, pp. 1037-1044.
- [17] D. Mazauric, S. Soltan, and G. Zussman, "Computational analysis of cascading failures in power networks," in Proceedings of the ACM SIGMETRICS/International Conference on Measurement and Modeling of Computer Systems, ser. SIGMETRICS '13. New York, NY, USA: ACM, 2013, pp. 337-338.
- [18] A. Bernstein, D. Bienstock, D. Hay, M. Uzunoglu, and G. Zussman, "Power grid vulnerability to geographically correlated failures 2014; analysis and control implications," in IEEE INFOCOM 2014 - IEEE Conference on Computer Communications, April 2014, pp. 2634-2642.
- [19] D. Bienstock and A. Verma, "The n-k problem in power grids: New models, formulations, and numerical experiments," SIAM Journal on Optimization, vol. 20, no. 5, pp. 2352-2380, 2010. A. Wood and B. Wollenberg, Power Generation, Operation, and Control.
- Wiley-Interscience, 1996.
- [21] D. Bienstock, "Optimal control of cascading power grid failures," in 2011 50th IEEE Conference on Decision and Control and European Control Conference, Dec 2011, pp. 2166-2173.
- [22] D. Bienstock and S. Mattia, "Using mixed-integer programming to solve power grid blackout problems," Discrete Optimization, vol. 4, no. 1, pp. 115 - 141, 2007, mixed Integer ProgrammingIMA Special Workshop on Mixed-Integer Programming.
- [23] F. R. K. Chung, Spectral Graph Theory. American Mathematical Society, 1997.
- [24] F. Dorfler and F. Bullo, "Kron reduction of graphs with applications to electrical networks," IEEE Transactions on Circuits and Systems I: Regular Papers, vol. 60, no. 1, pp. 150-163, Jan 2013.
- [25] N. M. M. de Abreu, "Old and new results on algebraic connectivity of graphs," Linear Algebra and its Applications, vol. 423, no. 1, pp. 53 -73, 2007.
- [26] R. Grone, R. Merris, and V. S. Sunder, "The laplacian spectrum of a graph," SIAM Journal on Matrix Analysis and Applications, vol. 11, no. 2, pp. 218-238, 1990.
- [27] R. Bhatia, Matrix Analysis. New York: Springer Verlag, 1997.
- C. Mavroforakis, R. Garcia-Lebron, I. Koutis, and E. Terzi, "Spanning edge centrality: Large-scale computation and applications, Proceedings of the 24th international conference on world wide web. International World Wide Web Conferences Steering Committee, 2015, pp. 732-742.
- S. Chaiken, "A combinatorial proof of the all minors matrix tree theorem," SIAM Journal on Algebraic Discrete Methods, vol. 3, no. 3, pp. 319-329, 1982.
- A. S. Teixeira, P. T. Monteiro, J. A. Carriço, M. Ramirez, and A. P. Francisco, "Spanning edge betweenness," in Workshop on mining and learning with graphs, vol. 24, 2013, pp. 27-31.